How does dense phase CO_2 influence the phase behaviour of block copolymers synthesised by dispersion polymerisation?

J. Jennings,[a] S. P. Bassett,[a] D. Hermida-Merino,[b] G. Portale, [b] W. Bras,[b] L. Knight,[a] J. J. Titman,[a] T. Higuchi,[c] H. Jinnai, [c] S. M. Howdle [a]

[a] *School of Chemistry, University of Nottingham, University Park, Nottingham, NG7 2RD, UK. E-mail: steve.howdle@nottingham.ac.uk; Fax: +0044 115 846 8459; Tel: +44 (0)115 9513486*

[b]*DUBBLE@ESRF, Netherlands Organisation for Scientific Research (N.W.O.), CS40220, 38043, Grenoble, Cedex 9, France*

[c] *Institute of Multidisciplinary Research for Advanced Materials (IMRAM), Tohoku University, 2-1-1 Katahira, Aoba-ku, Sendai 980-8577, Japan*

Abstract

Block copolymers synthesised in supercritical CO_2 dispersion undergo *in situ* self-assembly which can result in a range of nanostructured microparticles. However, our previous study revealed that copolymers with different block combinations possessed different microphase separated morphologies at identical block volume fractions. In this paper, we follow up those initial observations. By examining the phase behaviour of a selection of structurally diverse block copolymers, we explore the structural factors which influence the conflicting self-assembly behaviours. The composition dependence of the morphology is found to be strongly related to the CO_2-philicity of the second block relative to poly(methyl methacrylate) (PMMA). Whilst PMMA-*b*-poly(benzyl methacrylate) (PBzMA) and PMMA-*b*-poly(N,N-dimethylaminoethylmethacrylate) (PDMAEMA) phase behaviour follows traditional diblock copolymer phase diagrams, PMMA-*b*-poly(styrene) (PS) and PMMA-*b*-poly(4-vinyl pyridine) (P4VP), which comprise blocks with the greatest contrast in CO_2-philicity, self-assemble into unexpected morphologies at several different block volume fractions. The morphology of these copolymers in the microparticulate form was found to revert to the predicted equilibrium morphology when the microparticles were re-cast as films and thermally annealed. These findings provide strong evidence that CO_2 acts as a block-selective solvent during synthesis. The CO_2-selectivity was exploited to fabricate various kinetically trapped non-lamellar morphologies in symmetrical PMMA-*b*-PS copolymers by tuning the

ratio of polymer:CO_2. Our data demonstrate that CO_2 can be exploited as a facile process modification to control the self-assembly of block copolymers within particles.

Introduction

Block copolymer self-assembly is an important phenomenon that has facilitated the development of new areas of research and applications in material science.[1] The driving force for polymer-polymer phase separation is the enthalpic incompatibility of two or more chemically distinct polymers. In block copolymers, the presence of covalent bonds between the polymers prevents macrophase separation and results instead in microphase separated domains typically on the order of 10-100 nm in size. To achieve self-assembly in diblock copolymers, the two blocks must have a sufficiently high Flory-Huggins interaction parameter (χ), and degree of polymerisation (N). Through theoretical and experimental studies, it has been elucidated that the product χN must exceed a critical value of ~10.5 in order for a diblock copolymer to overcome the entropic penalty of chain stretching and microphase separate.[2] The appearance of the morphology depends on the relative block volume fraction (f) of the two blocks, the most common being lamellar, bicontinuous (e.g. double gyroid[3] or double diamond[4]), hexagonally-packed cylinders and body centered cubic spherical phase, listed in order of deviation from flat interfacial curvature. These diverse structures and the length-scales at which they exist have been exploited for many nanotechnology applications including nanocomposite synthesis,[5] bottom up lithography[6] and photonic crystals.[7]

Confinement of self-assembled block copolymers in three dimensions (i.e. in nano or microparticles, nanorods etc.) has further expanded the field and potential scope of applications. In addition to conventional morphologies, new frustrated structures have been observed in block copolymer nanoparticles including mushroom, screw-like and helical morphologies which occur when the size of the confining particle approaches the range of block domain sizes.[8, 9] Block copolymer particles have inspired investigations into a range of functional materials for use in drug delivery,[10, 11] synthesis of mesostructured inorganic materials[12], bio-imaging[13] and metamaterials.[14]

A number of methods exist for the fabrication of microphase separated block copolymer particles. The most common techniques to date are those which exploit solvent evaporation-

induced self-assembly. For example, the self-organised reprecipitation (SORP) method involves slow solvent evaporation from block copolymer dissolved in a solvent/non-solvent mixture. This results in block copolymer particles formed by precipitation, in which self-assembly can be induced either by means of solvent[15] or thermal annealing.[16] Other related methods exploit solvent evaporation from block copolymers dissolved in dispersed particles[17] or aerosols.[11, 18] However, the drawbacks of these methods include the requirement for multiple steps (i.e. block copolymer synthesis followed by solvent evaporation and annealing) and the use of volatile organic solvents. An alternative route is the use of emulsion, miniemulsion or dispersion polymerisations in which block copolymers are synthesised and self-assembly occurs within the particle during polymerisation. These techniques typically exploit controlled radical polymerisation (CRP) techniques in green solvents including water[19-21] and supercritical carbon dioxide ($scCO_2$).[22, 23] Solvophobic polymerisations provide an attractive route to block copolymer microparticles since they are relatively facile, green and industrially applicable with fewer processing steps. However, both green solvents have drawbacks: water consumes significant energy in drying and waste water must be cleaned up after use; and $scCO_2$ requires specialised high pressure equipment.[24]

Recently we reported a route to block copolymers which takes advantage of the excellent livingness of RAFT polymerisation in a dispersion polymerisation in $scCO_2$. This proved to be a particularly effective method to access a range of block copolymer particles with a wide array of nanostructured morphologies.[22, 23] Understanding the factors governing the phase behaviour of block copolymer particles synthesised in $scCO_2$ is crucial for establishing structure-property relationships for the design of new materials for novel applications. Herein we investigate the possible influence of CO_2 on the morphology of several block copolymers synthesised by dispersion polymerisation in the medium. The equilibrium structure of the block copolymers was studied by preparing solution cast films, and further insight into the effect on the morphology by CO_2 was gained by modulating the polymer:CO_2 ratio through adjustment of monomer loading. The results provide insight into the mechanism of formation, and possible new methods by which to exert control of block copolymer morphology within microparticles.

Experimental

Block copolymer structural characterisation

The block copolymer synthetic procedure is outlined in the supporting information. Block copolymers were analysed by ^{1}H NMR in $CDCl_3$ on a Bruker DPX 300 MHz spectrometer in order to determine the mass fraction of the blocks. This was converted to volume fraction, f_{PMMA}, using the melt densities, where available (PMMA (1.17 g cm^{-3}), PBzMA (1.179 g cm^{-3}), PS (1.05 g cm^{-3}) and P4VP (1.15 g cm^{-3})).[25] Molecular weight ($M_{n,exp}$) and dispersity (Đ) were determined by GPC using either an Agilent PL GPC 120 in THF or a PL GPC 50 in a mixture of chloroform/ethanol/triethylamine (90/10/0.5 by volume). Analyses were run at a flow rate of 1 mL min^{-1} and 40 °C, and columns were calibrated with PMMA narrow standards.

Transmission electron microscopy (TEM)

Block copolymer particles were embedded in epoxy resin (Agar 100) and set at 35 °C for 72 h before being ultramicrotomed at room temperature to ~100 nm slices with a diamond knife (Leica Diatome Ultra 45°) and collected on copper grids. Sections of PMMA-*b*-PBzMA were stained with RuO_4 for ~1 h, which adsorbs selectively to PBzMA domains. PMMA-*b*-PSt particles were stained prior to resin embedding with OsO_4 for 24 h, which adsorbs selectively to PS. Sections of PMMA-*b*-P4VP and PMMA-*b*-PDMAEMA were stained with I_2 vapour for ~2 h, which selectively adsorbs to P4VP and PDMAEMA domains. Imaging of particle samples took place on either a JEOL 200FXII or a FEI Tecnai microscope.

Block copolymer films were prepared by solvent casting. PMMA-*b*-PS and PMMA-*b*-PBzMA particles were dissolved in toluene at 1 wt% and cast as films before being annealed at 160 °C *in vacuo* for 2 days. PMMA-*b*-P4VP particles were dissolved in chloroform at 2 wt% and cast as films, before being annealed in a saturated atmosphere of chloroform vapour. The films were then embedded in an acrylic resin and ultramicrotomed at room temperature with a diamond knife. Sections were collected on copper grids and stained with RuO_4 (PMMA-*b*-PBzMA and PMMA-*b*-PS) or I_2 (PMMA-*b*-P4VP) for 8 h. TEM imaging of the films was conducted at 200 kV.

Small Angle X-ray Scattering (SAXS)

SAXS data were collected at the ESRF (Grenoble) at a sample-to-detector distance of either ~3 m or 6.150 m with a wavelength of 1.033 or 0.8266 Å, respectively. A Dectris-Pilatus 1M detector with a resolution of 981 x 1043 pixels and a pixel size of 172 x 172 μm was employed to record the 2D scattering profiles. Standard corrections for sample absorption and background subtraction were performed. The data were normalised with respect to the incident beam intensity in order to correct for primary beam intensity fluctuations. The scattering patterns from rat tail collagen or silver behenate were used for the calibration of the wave vector scale of the scattering curve. Bulk films or neat block copolymer particles were placed in the beamline and SAXS patterns were acquired at room temperature. The scattering vector q is defined as $q = 4\pi/\lambda \sin\theta$, where 2θ is the scattering angle. Domain spacing, D, was calculated from $D = 2\pi/q_{max}$, where q_{max} is the position of the principle scattering peak.

Solid State NMR (SS NMR)

SS NMR data were acquired on a Bruker Avance III spectrometer operating at 600.13 MHz using a 1.3 mm HX MAS probe with a spinning rate of 60 kHz. A simple three-pulse exchange pulse sequence was used to acquire two-dimensional ^{1}H-^{1}H spin diffusion spectra. The spectral width in both dimensions was set to 50 ppm. To obtain a complete diffusion profile between 13-17 spectra were acquired for each sample using mixing times of duration 1 ms to 700 ms. Pure phase lineshapes were obtained using TPPI, and a z-alternation phase cycle was used, as described by Spiess and Schmidt-Rohr.[26] The relaxation delay was between 5 and 7 s depending on the sample, so that the total acquisition time for a single 2D ^{1}H-^{1}H spin diffusion spectrum was around 3 hours.

Deconvolution of the spectra was carried out by fitting 16 two-dimensional peaks to the 2D data surface using mixed Lorentzian/Gaussian peak shapes with fixed positions and varying widths and amplitudes. Intensities were obtained by taking the volume integrals of the fitted peaks. These were corrected for T1 relaxation and then normalised against the total magnetisation present at short mixing times. The change intensity of the polystyrene aromatic diagonal peak showed two linearly decaying regions corresponding to intra-domain and inter-domain spin diffusion. The second shallower decay was extrapolated to the time taken for full equilibration of the magnetisation and this time was then used to calculate a domain size according to the methods described by Spiess and co-workers.[26, 27] T1 values were recorded for all samples using separate saturation-recovery experiments. Simple one-dimensional spectra were recorded to obtain the equilibrium magnetisation levels.

To obtain an independent measure of the spin diffusion coefficients in the two polymer domains, average distances between different ^{1}H sites in a single repeating unit were calculated using QChem.[28] The average difference between the PS aromatic and the aliphatic hydrogens was 0.50 nm and the average distance between the PMMA methoxy and methyl hydrogens was 0.56 nm.

Results and Discussion

A series of PMMA-containing block copolymers were synthesised in $scCO_2$ dispersion.[22, 23] Efficient RAFT control over MMA polymerisation was demonstrated, with PMMA dispersity in the range 1.2-1.5. Chain extension to block copolymer was observed by the increase in molecular weight by GPC, while dispersity remained relatively low (mostly <1.7). As previously, higher dispersities were recorded for some PMMA-b-PS and PMMA-b-P4VP copolymers, where termination during the second block polymerisation occurred by combination and lead to a high molecular weight shoulder in the GPC trace (SI Figure 1). Second blocks were selected that differed in CO_2-philicity: from the more CO_2-philic poly(benzyl methacrylate) (PBzMA) and poly(N,N-dimethylaminoethyl methacrylate) (PDMAEMA), to the more CO_2-phobic polystyrene (PS) and poly(4-vinylpyridine) (P4VP). Block copolymer particles with a range of block volume fractions and molecular weights were synthesised *via* dispersion polymerisation in $scCO_2$ to understand the effect of $scCO_2$ on the final particle internal morphology.

A comparison of the morphology within particles obtained directly from $scCO_2$ and after thermal annealing was then carried out to probe the persistence of the obtained structure. Furthermore, the equilibrium structure of the block copolymers was studied by preparing solution cast films and correlating the morphologies obtained with literature examples of these block copolymers synthesised by standard methods. Finally, to gain further insight into the effect on the morphology by CO_2, the polymer to CO_2 ratio was varied by synthesising block copolymers at different monomer loadings.

Block copolymers with various volume fractions were synthesised targeting two molecular weights by a RAFT-controlled dispersion polymerisation and morphology investigated through TEM analysis (Table 1). Polymers are named according to the theoretical number

average molecular weights of the two blocks in the copolymer, e.g. $PMMA_x$-$P2_y$, where x and y represent the target molecular weight of PMMA and block P2 in the copolymer (in kg mol^{-1}), calculated from the molar ratio of monomer to RAFT agent used in the synthesis.

Table 1: Characteristics of block copolymers synthesised by RAFT dispersion in $scCO_2$ for phase behaviour studies

Block copolymer name	$M_{n,exp}$ [a] ($/10^3$ g mol^{-1})	Đ[a]	f_{PMMA} [b]	Morphology[c]
$PMMA_{22.5}$- $PBzMA_{37.5}$	54	1.60	0.39	LAM
$PMMA_{30}$-$PBzMA_{30}$	57	1.53	0.51	LAM/DIS
$PMMA_{37.5}$-$PBzMA_{22.5}$	55	1.24	0.61	LAM/CYL
$PMMA_{45}$-$PBzMA_{15}$	51	1.35	0.72	SPH/DIS
$PMMA_{37.5}$-$PBzMA_{62.5}$	73	1.26	0.38	LAM
$PMMA_{50}$-$PBzMA_{50}$	77	1.38	0.51	LAM
$PMMA_{62.5}$-$PBzMA_{37.5}$	73	1.66	0.64	LAM/BIC
$PMMA_{75}$-$PBzMA_{25}$	70	1.45	0.78	SPH
$PMMA_{30}$-$PDMAEMA_{30}$	44	1.33	0.58	LAM
$PMMA_{45}$-$PDMAEMA_{15}$	48	1.24	0.83	CYL
$PMMA_{22.5}$-$PS_{37.5}$	55	1.42	0.36	LAM
$PMMA_{30}$-PS_{30}	54	1.69	0.48	CYL
$PMMA_{37.5}$-$PS_{22.5}$	46	1.67	0.61	SPH
$PMMA_{45}$-PS_{15}	49	1.81	0.76	SPH
$PMMA_{37.5}$-$PS_{62.5}$	71	1.57	0.38	LAM
$PMMA_{50}$-PS_{50}	73	1.83	0.48	SPH
$PMMA_{62.5}$-$PS_{37.5}$	68	1.93	0.61	SPH
$PMMA_{75}$-PS_{25}	71	1.97	0.77	SPH
$PMMA_{15}$-$P4VP_{45}$	61	1.71	0.67	LAM
$PMMA_{30}$-$P4VP_{30}$	68	1.98	0.49	SPH
$PMMA_{45}$-$P4VP_{15}$	69	1.99	0.29	SPH

[a]Derived from GPC analysis in THF (PMMA-b-PBzMA and PMMA-b-PS) or $CHCl_3$/EtOH/TEA (PMMA-b-PDMAEMA and PMMA-b-P4VP) analysed against PMMA standards. [b]Calculated from the weight fraction of PMMA derived from ^{1}H NMR analysis. [c]Determined by TEM imaging: LAM (lamellar), BIC (bicontinuous), CYL (cylindrical), SPH (spherical) and DIS (disordered morphology) or combinations thereof

All-methacrylic block copolymers

PMMA-*b*-PBzMA copolymer particles synthesised with different volume fractions in $scCO_2$ displayed a multitude of morphologies (Figure 1), ranging from lamellar to bicontinuous, cylindrical and spherical (in the latter two PMMA comprises the matrix), as the final volume fraction of PMMA in the copolymer increased. TEM imaging revealed evidence of the coexistence between nanostructured and disordered particles within certain PMMA-*b*-

PBzMA copolymer samples (SI Figure 2). SAXS analysis was conducted in order to investigate whether the majority of particles within the sample existed in the nanostructured or disordered state (SI Figure 3). The absence of any Bragg scattering in $PMMA_{30}$-$PBzMA_{30}$ and $PMMA_{45}$-$PBzMA_{15}$, leads us to believe that these samples consisted of mostly disordered particles (as notified in Table 1), signifying that PMMA-*b*-PBzMA was in the weak segregation limit and blocks are highly miscible at this molecular weight. The only other literature in which PMMA-*b*-PBzMA was studied by TEM found that a copolymer of ~15 kg mol^{-1} (synthesised in a heterogeneous polymerisation) was miscible and also formed disordered block copolymer particles.[29]

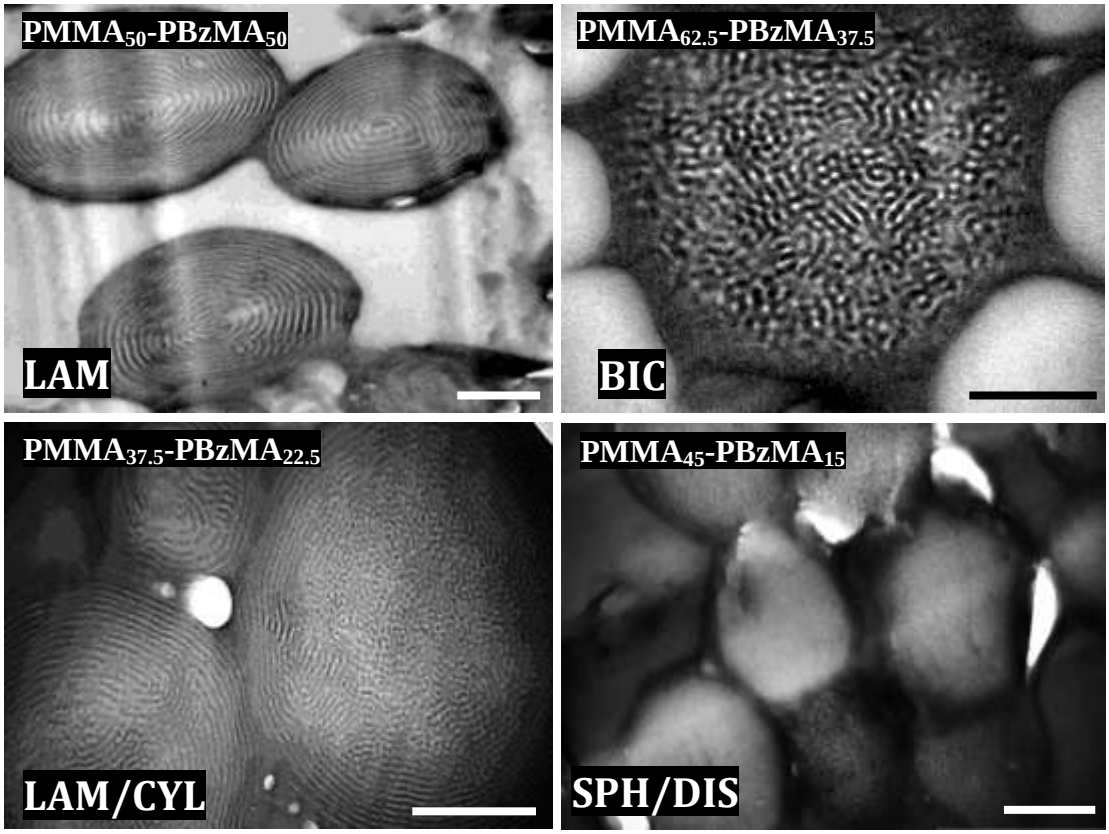

Figure 1: TEM images of cross-sectioned PMMA-b-PBzMA particles prepared at different final volume fractions and molecular weights, displaying a variety of morphologies: Lamellar (LAM), bicontinuous (BIC), lamellar/cylindrical coexistence (LAM/CYL) and spherical/disorder coexistence (SPH/DIS). The scale bar in all images is 500 nm.

The order and final volume fraction at which the different phases formed in PMMA-*b*-PDMAEMA was consistent with those in PMMA-*b*-PBzMA. The symmetrical copolymer

self-assembled into lamellar morphology, whilst cylindrical morphology (in which PMMA comprised the matrix) formed at a higher PMMA block volume fraction (Figure 2).

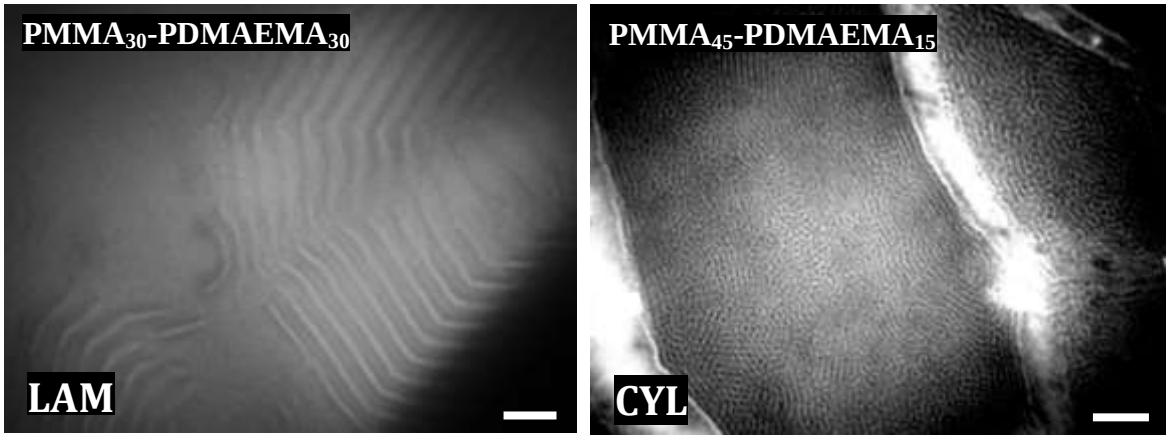

Figure 2: TEM images of cross-sectioned PMMA-b-PDMAEMA particles prepared at different final volume fractions and molecular weights, displaying a variety of morphologies: Lamellar (LAM) and cylindrical (CYL). The scale bar in both images is 200 nm.

The morphologies observed by TEM for PMMA-*b*-PBzMA were plotted in the form of an experimental phase diagram (Figure 3). The appearance of self-assembled morphologies at their respective block volume fractions suggested that PMMA-*b*-PBzMA (and PMMA-*b*-PDMAEMA) adhered to traditional behaviour of linear diblock copolymers. Thus, it appeared that these block copolymers synthesised in dispersion polymerisation in $scCO_2$ were minimally perturbed from equilibrium.

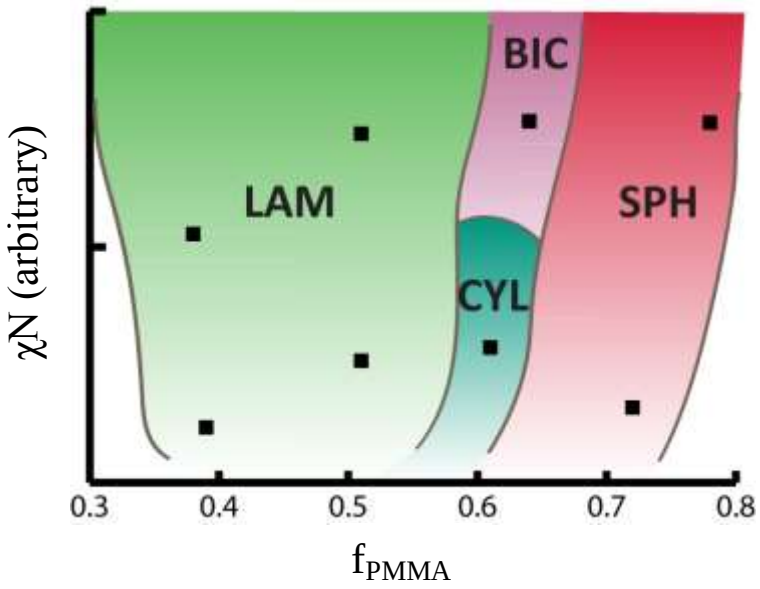

Figure 3: Experimental phase diagram for PMMA-b-PBzMA synthesised in scCO₂, constructed based on TEM images of block copolymers in Table 1. Block copolymers observed in this study (■) are plotted as a function of their relative degree of polymerisation (no χ interaction parameter data were available for this polymer pair) against calculated block volume fraction. Morphologies are abbreviated to LAM (lamellar), BIC (bicontinuous), CYL (cylindrical), SPH (spherical).

Methacrylic-styrenic block copolymers

The phase behaviour of PMMA-*b*-PS has been well studied in the literature in thin films and bulk,[30, 31] and under spherical confinement within microparticles formed *via* SORP.[32] Thus, this system provides an ideal opportunity to elucidate any effects that are specific to block copolymer structures produced in $scCO_2$. In particular, the higher CO_2-philicity of PMMA over PS is well-founded.[33] Characterisation by TEM revealed a range of morphologies from lamellar to cylindrical and spherical (in which PMMA comprised the matrix) as PMMA block volume fraction increased (Figure 4). Unlike PMMA-*b*-PBzMA, only one copolymer ($PMMA_{45}$-PS_{15}) showed coexistence of nanostructured and disordered particles, and the appearance of a strong Bragg peak in SAXS analysis suggested that the sample comprised nanostructured particles as the majority (SI Figure 4).

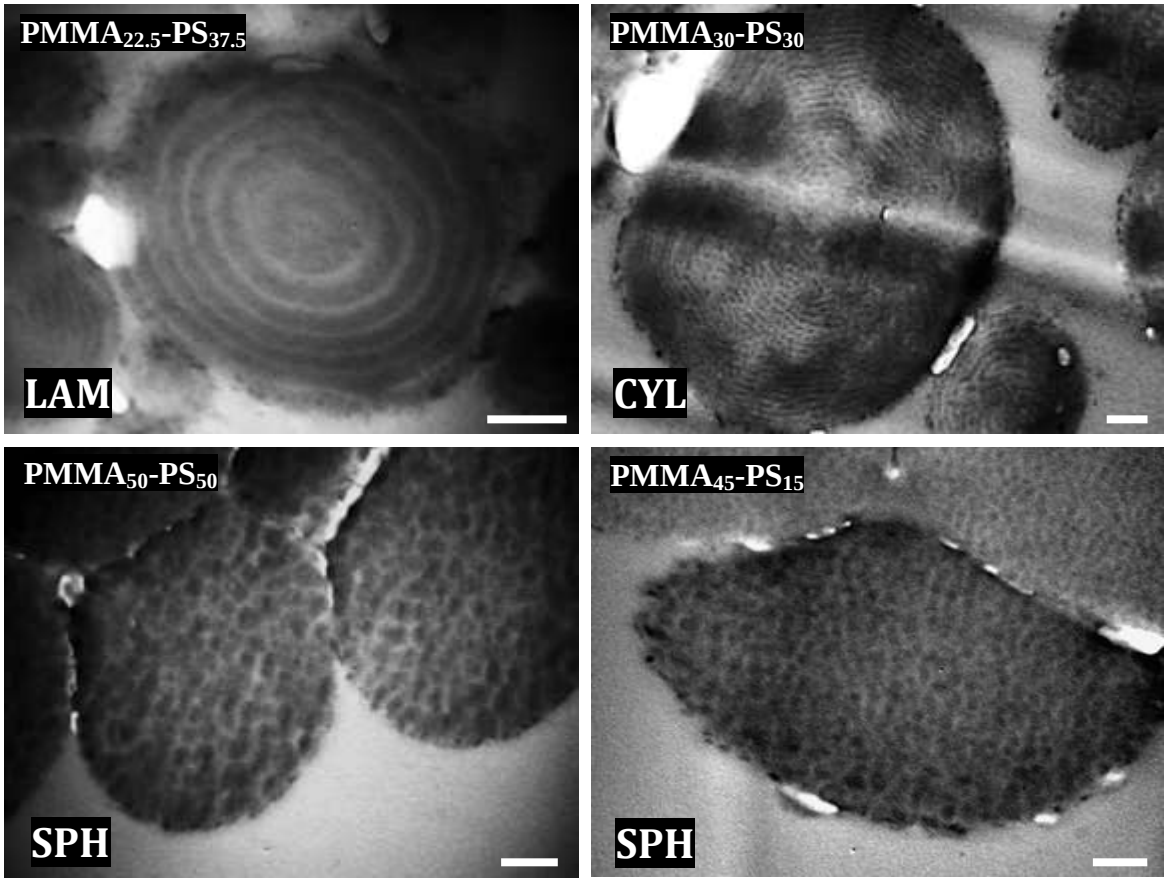

Figure 4: TEM images of cross-sectioned PMMA-b-PS particles prepared at different final volume fractions and molecular weights, displaying a variety of morphologies: Lamellar (LAM), cylindrical (CYL) and spherical (SPH). The scale bar in all images is 200 nm.

The experimental phase diagram (Figure 5) clearly revealed that the phase behaviour for PMMA-*b*-PS deviated from PMMA-*b*-PBzMA and PMMA-*b*-PDMAEMA, and from PMMA-*b*-PS reported previously. In our study, the symmetrical $PMMA_{50}$-*b*-PS_{50} (f_{PMMA} = 0.48) with total molecular weight of 73 kg mol^{-1} showed spherical morphology. Lamellar morphology has been widely observed in films and particles of PMMA-*b*-PS at comparable molecular weights and volume fractions[30, 32, 34]

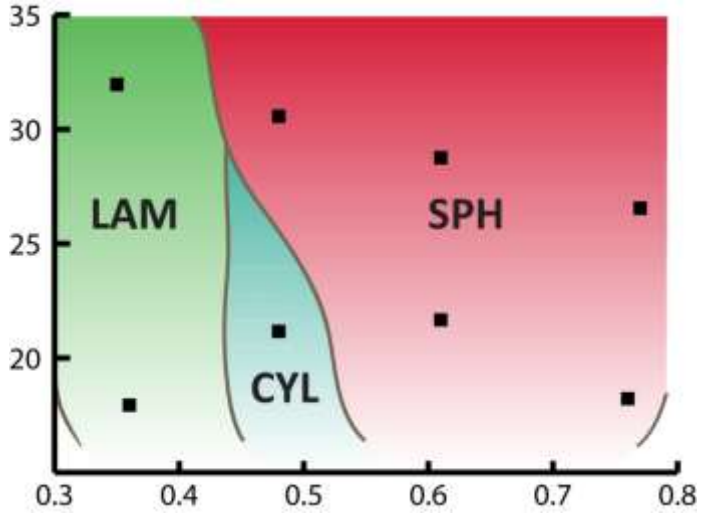

χN

f_{PMMA}

Figure 5: Experimental phase diagram for PMMA-b-PS synthesised in $scCO_2$, constructed based on TEM images of block copolymers in Table 1. Block copolymers observed in this study (■) are plotted as a function of χN using literature values of χ for PMMA-b-PS at 65 °C.[35] *Morphologies are abbreviated to L (lamellar), C (cylindrical) and S (spherical). The drastically different appearance to the phase diagram of PMMA-b-PBzMA strongly suggests that CO_2 is affecting the phase behaviour of these structurally distinct copolymers.*

TEM imaging of PMMA-*b*-P4VP (Figure 6) revealed phase behaviour more consistent with PMMA-*b*-PS than PMMA-*b*-PBzMA or PMMA-*b*-PDMAEMA. In particular, the symmetrical copolymer (f_{PMMA} = 0.49) showed spherical morphology (in which PMMA formed the matrix), whilst the more P4VP-rich copolymer (f_{PMMA} = 0.29) showed lamellae.

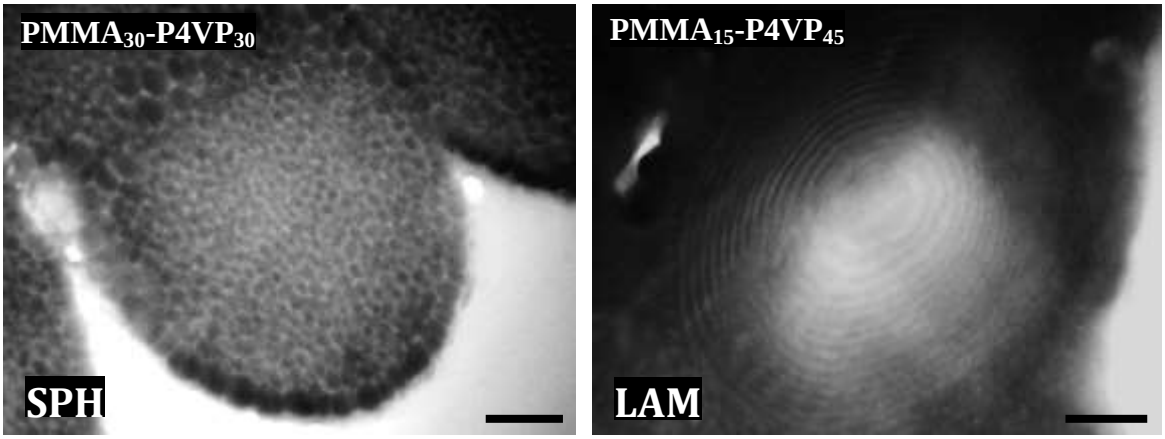

Figure 6: TEM images of cross-sectioned PMMA-b-P4VP particles prepared at different final volume fractions, displaying a variety of morphologies: spherical (SPH) and lamellar (LAM). The scale bar in all images is 200 nm.

Block copolymer annealing

Comparison of phase behaviour of all methacrylic vs. methacrylic-styrenic block copolymers confirmed that block volume fraction is not the only factor influencing phase behaviour of block copolymers synthesised in $scCO_2$ dispersion. In particular, the morphologies formed in methacrylic-styrenic copolymers were more curved away from PMMA at the same volume fractions. The methacrylic-styrenic copolymers differed from all methacrylics in that they displayed higher dispersities, and also higher homopolymer contamination, as estimated by chromatography in our previous report.[23] Block dispersity has been observed to influence diblock copolymer self-assembly, resulting in morphologies with increased curvature toward the more polydisperse domain.[36] In addition to this, homopolymer contamination could lead to discrepancies in block volume fraction which could also explain the deviations in phase behaviour for the methacrylic-styrenic copolymers.

Thus, to investigate whether structural variables caused the deviation in block copolymer phase behaviour, solvent cast bulk films were prepared from the $scCO_2$ synthesised particles to effect a more thermodynamically stable state of the various block copolymers (Figure 7).

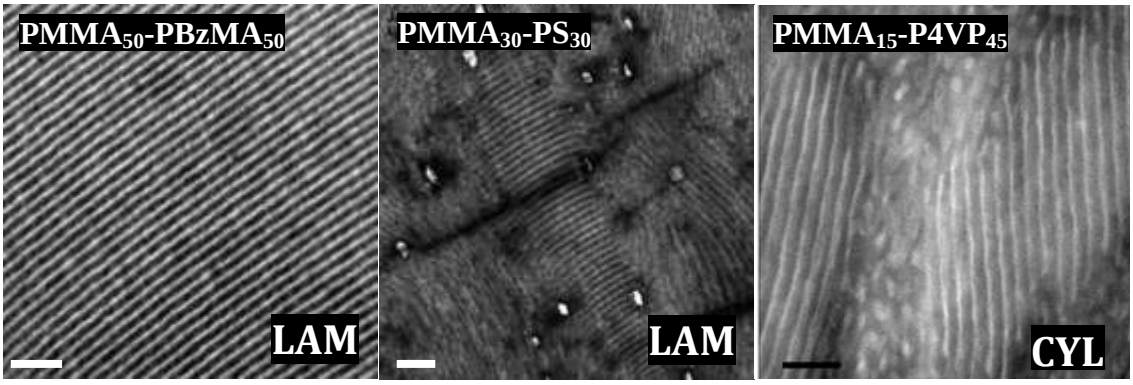

Figure 7: TEM images of block copolymer bulk films prepared by directly solvent casting and annealing the $scCO_2$ synthesised microparticles. Scale bar in each image is 200 nm.

In the symmetrical $PMMA_{50}$-$PBzMA_{50}$, the bulk film displayed lamellar morphology, consistent with the as-synthesised particles (Figure 1). However, the symmetrical block copolymer of $PMMA_{30}$-PS_{30}, which displayed cylindrical morphology in microparticles (Figure 4), showed lamellar morphology in the film. Finally, $PMMA_{15}$-$P4VP_{45}$, which had lamellar morphology in the particles (Figure 6), showed a disordered cylindrical morphology,

in which P4VP was the matrix, in the bulk film form. Due to the slightly ambiguous nature of the TEM image of $PMMA_{15}$-$P4VP_{45}$ film, SAXS analysis was also performed in order to confirm the assignment (SI Figure 5). Overall, the observed bulk film morphologies were consistent with traditional block copolymer self-assembly. The morphology of the symmetrical PMMA-*b*-PS in particles has also been found to be lamellar, which rules out the possibility of spherical confinement influencing the phase behaviour.[32] Frustration arising from spherical confinement is typically observed when the ratio of particle diameter to domain spacing is smaller than 2,[8] a ratio which we far exceed in our present study. Clearly, the morphologies that we obtained in the microparticles directly from $scCO_2$ are kinetically trapped, and thermodynamically-stable morphologies are only obtained after these particles have been dissolved and then solvent cast into bulk films. This strongly indicates that the contrast in CO_2-philicity was influencing phase behaviour in these block copolymer systems.

Although $scCO_2$ is the non-solvent for dispersion polymerisation, it is absorbed by many polymers, resulting in a swelling and plasticisation.[37] Thus, it likely has some influence on the dispersed particles of block copolymer synthesised *in situ*. Studies into block copolymer phase behaviour in the presence of CO_2 yield often conflicting results. In some cases, the miscibility of the two blocks is increased, as unfavourable enthalpic interactions are screened by CO_2 sorption.[38] In block copolymers with lower disorder-order transitions (LDOT), CO_2 sorption can lower the temperature at which phase separation occurs by increasing compressibility of polymer chains, which entropically disfavours mixing.[39] Finally, order-order transitions (OOTs) can be affected when the superior solubility of CO_2 in a CO_2-philic block (e.g. fluorinated or siloxane polymers) results in an increase in effective block volume fraction and hence a phase transition[40-42]. We speculated that the polymer structure-dependent solubility of CO_2 influenced the phase behaviour of methacrylic-styrenic block copolymers relative to all methacrylics in the manner of a block selective solvent during the synthesis.[22]

Domain size measurements

In addition to SAXS and TEM measurements, solid-state NMR spin diffusion experiments were carried out to obtain an additional measure of the average domain size throughout the whole sample. Ultrafast magic angle spinning (MAS) ^{1}H – ^{1}H two-dimensional exchange spectra were recorded with increasing mixing times[43], and the changes in peak intensities were used to monitor the transfer of magnetization between the domains by spin diffusion. This approach can be applied here, because the two domains are rigid, so that the spin-lattice

relaxation times are relatively long. Figure 8 shows the resulting decay in the intensity of the diagonal peak in the two-dimensional spectrum corresponding to the polystyrene aromatic ^{1}H sites for three samples: $PMMA_{37.5}$-$PS_{22.5}$, $PMMA_{62.5}$-$PS_{37.5}$ and $PMMA_{50}$-PS_{50}. The initial steep decay results from the re-equilibration of magnetization between side-group aromatic and backbone aliphatic sites within the PS blocks, while the subsequent shallower decay occurs as magnetization is transferred to the PMMA domains. For the latter the time taken for the magnetisation to decay to its equilibrium value is related to the domain size of the polymer which can be calculated using the method previously described by Speiss.[26, 27] The resulting domain sizes are compared with those obtained from SAXS and TEM in Table 2. Further experimental details are given in the Supplementary Information).

To further probe the kinetically-trapped nature of the morphologies observed in PMMA-*b*-PS particles, samples were thermally annealed above the glass transition temperature (T_g), but below the order-disorder transition temperature. This processing imparted polymer mobility to facilitate the return to the preferred block copolymer morphology in the absence of CO_2. A number of PMMA-*b*-PS samples were analysed by SAXS before and after thermal annealing experiments. The position of Bragg reflections at similar q values before and after thermal treatment suggested that no major morphological shifts (i.e. order-order transitions) took place, although this could not be confirmed due to the lack of higher order peaks. This implied that microphase separation remained localised within particles, and no long range order developed during the annealing experiment.

Interestingly, an increase in domain size was registered after thermal treatment for PMMA-*b*-PS particles at all volume fractions and molecular weights (measured by SAXS only). Since the domain spacing in a block copolymer is proportional to χN, the smaller domain size in the as-synthesised particles could be a result of the decrease in χ by CO_2. A decrease in χ for block copolymers annealed in CO_2 has been previously reported, and can be explained by block miscibilisation.[38] Thus, CO_2 was most likely decreasing χ between PMMA and PS, affecting smaller domain sizes, which further hinted that a kinetically-trapped morphology synthesised in $scCO_2$ was returning to the thermodynamically favoured state over the course of the annealing experiment.

Table 2: PMMA-*b*-PS domain size measurements before and after thermal annealing

Block Copolymer	Morphology[a]	D_{TEM}[a] (nm)	D_{NMR}[b] (nm)	D_{SAXS}[c] (nm)	$D_{SAXS\ annealed}$[c] (nm)
$PMMA_{22.5}$-$PS_{37.5}$	LAM	33	24	37	40
$PMMA_{30}$-PS_{30}	CYL	35	38	39	n/a
$PMMA_{37.5}$-$PS_{22.5}$	SPH	41	33	39	40
$PMMA_{45}$-PS_{15}	SPH	44	30	25	29
$PMMA_{37.5}$-$PS_{62.5}$	LAM	48	50	54	59
$PMMA_{50}$-PS_{50}	SPH	76	60	62	n/a
$PMMA_{62.5}$-$PS_{37.5}$	SPH	55	41	49	53
$PMMA_{75}$-PS_{25}	SPH	55	41	46	48

[a]Determined by TEM imaging: LAM (lamellar), CYL (cylindrical), SPH (spherical). [b]Calculated from solid state NMR ^1H-^1H spin diffusion spectra; [c]Derived from the principal scattering peak (q_{max}) in the SAXS profile using $D = 2\pi/q_{max}$

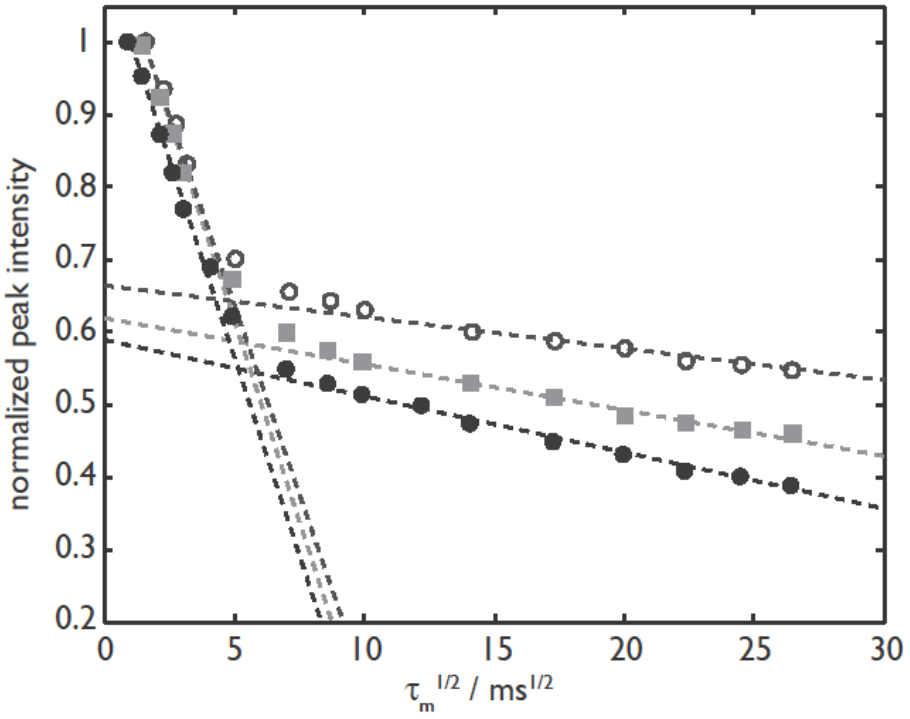

Figure 8. Decay of the diagonal peak corresponding to aromatic PS ^1H sites from ultrafast MAS ^1H - ^1H two-dimensional exchange NMR spectra as a function of mixing time τ_m for three copolymers: $PMMA_{37.5}$-$PS_{22.5}$ (filled circles) $PMMA_{62.5}$-$PS_{37.5}$ (grey squares) and $PMMA_{50}$-PS_{50} (open circles). The lines show linear extrapolations used to find the mixing time when re-equilibration is achieved, from which the domain size can be extracted.

Block copolymers synthesis at variable monomer loading

In the presence of a selective solvent, block copolymer self-assembly is influenced by the volume fraction of block copolymer relative to solvent.[44] Increasing the concentration of a selective solvent enhances swelling and therefore effective volume fraction of one block, resulting in morphologies with increasing curvature away from the block for which the solvent is selective. By synthesising block copolymers at different monomer loading, the volume fraction of the final copolymer in CO_2, $\Phi_{copolymer}$, could be adjusted. Symmetrical PMMA-*b*-PBzMA and PMMA-*b*-PS copolymers were synthesised at two monomer loadings, targeting two molecular weights, and the phase behaviour studied by TEM (Table 3, Figures 9 and 10).

Table 3: Characteristics of block copolymers synthesised by RAFT dispersion in scCO$_2$ at various monomer loadings

Block copolymer name	$M_{n,exp}$[a] (/10^3 g mol^{-1})	Đ[a]	$\Phi_{copolymer}$[b]	Morphology[c]
$PMMA_{30}$- $PBzMA_{30}$-16ml	54	1.60	0.225	LAM/DIS
$PMMA_{30}$-$PBzMA_{30}$-25ml	57	1.53	0.347	LAM/DIS
$PMMA_{50}$-$PBzMA_{50}$-16ml	77	1.38	0.225	LAM
$PMMA_{50}$-$PBzMA_{50}$-25ml	92	1.24	0.347	LAM
$PMMA_{30}$-PS_{30}-16ml	55	1.42	0.237	CYL
$PMMA_{30}$-PS_{30}-25ml	54	1.69	0.367	LAM
$PMMA_{50}$-PS_{50}-16ml	77	1.86	0.237	SPH
$PMMA_{50}$-PS_{50}-25ml	91	1.48	0.367	CYL

[a]Derived from GPC analysis in THF (PMMA-b-PBzMA and PMMA-b-PS) or analysed against PMMA standards. [b]Calculated from $\Phi_{copolymer} = (v_{MMA} + v_{monomer\text{-}2}) / (v_{CO_2} + v_{MMA} + v_{monomer\text{-}2})$ *[c]Determined by TEM imaging: LAM (lamellar), CYL (cylindrical), SPH (spherical) and DIS (disordered)*

For PMMA-*b*-PBzMA, the expected lamellar morphology was observed at both molecular weights and regardless of $\Phi_{copolymer}$ (Figure 9). For a block copolymer in a neutral solvent, morphology should remain constant with $\Phi_{copolymer}$.[45] This suggests an equal swelling of the

structurally similar methacrylate blocks by CO_2 and no influence on relative block volume fractions, as expected.

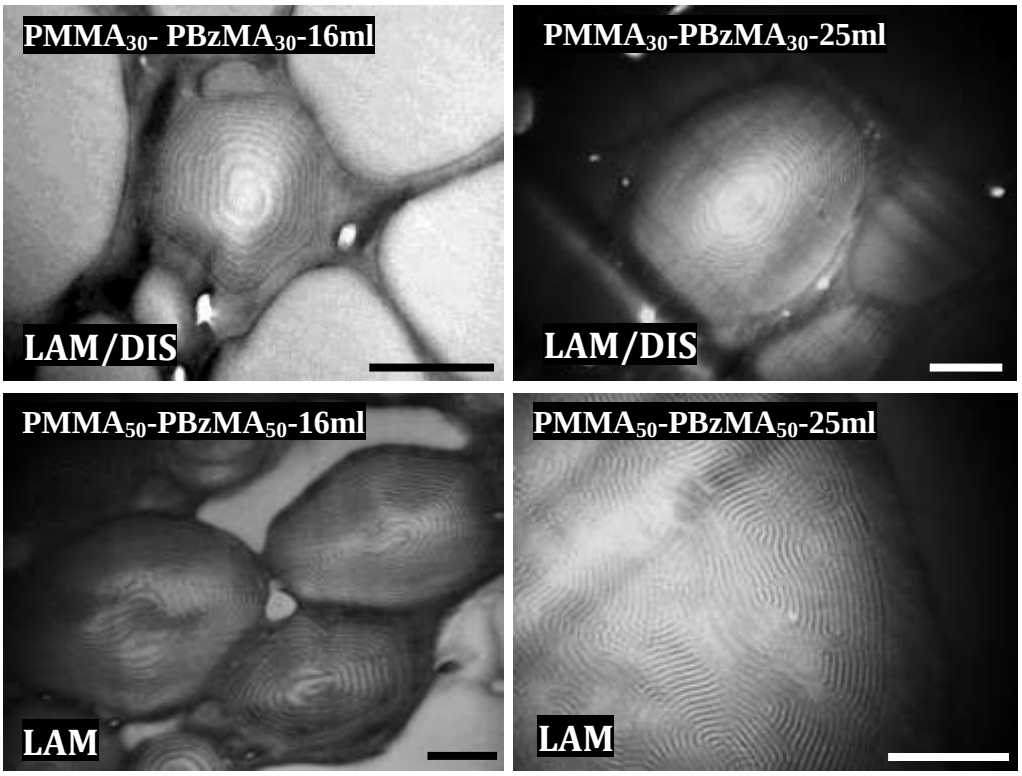

Figure 9: TEM images of cross-sectioned particles of $PMMA_{30}$-$PBzMA_{30}$ (top) and $PMMA_{50}$-$PBzMA_{50}$ (bottom) synthesised at two polymer volume fractions in CO_2 ($\Phi_{copolymer}$). Scale bar in all images is 500 nm. Morphology was evidently independent of the polymer concentration in CO_2.

On the contrary, particles synthesised under the same conditions for PMMA-*b*-PS showed a polymer volume fraction-dependent morphology at both molecular weights (Figure 10). Specifically, as $\Phi_{copolymer}$ increased, a transition from cylindrical to lamellar morphology occurred for $PMMA_{30}$-PS_{30} (Figure 10, top) and spherical to cylindrical for $PMMA_{50}$-PS_{50} (Figure 10, bottom).

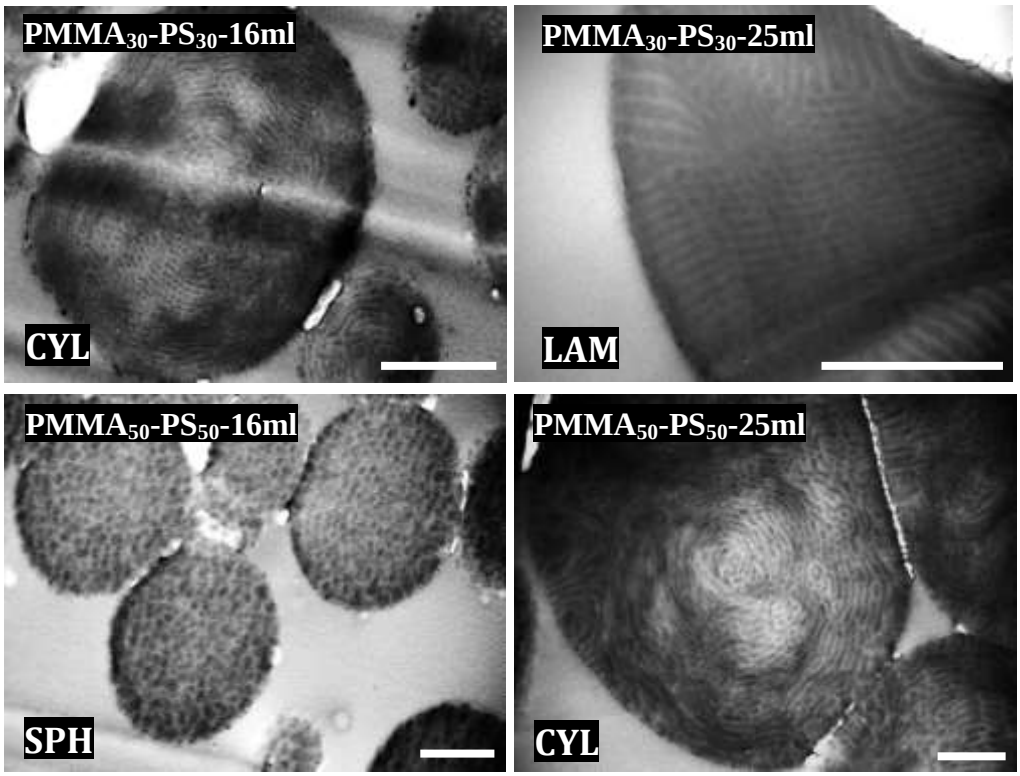

Figure 10: TEM images of cross-sectioned particles of $PMMA_{30}$-PS_{30} (top) and $PMMA_{50}$ – PS_{50} (bottom) synthesised at two polymer volume fractions in CO_2 ($\Phi_{copolymer}$). Scale bar in all images is 500 nm. Morphology was heavily influenced by polymer concentration in CO_2.

As $\Phi_{copolymer}$ was decreased (i.e. CO_2 concentration increased), the morphology shifted across the phase diagram towards phases which were more highly curved away from PMMA. This is consistent with selective swelling of PMMA. The fact that CO_2 is selective for methacrylates over styrenics is well known, and numerous reports have quantified a greater degree of CO_2 absorbed and thus volume increase in such polymers.[33] This is thought to be a result of Lewis base-Lewis acid interactions between the carbonyl oxygen lone pair and the electropositive carbon in CO_2.[46] This degree of relative volume increase can be controlled by varying the polymer volume fraction in CO_2, which materialises in a shift in self-assembled morphology. This is likely also the cause of the shifted phase behaviour in the structurally related PMMA-*b*-P4VP copolymer system,

The fact that the non-equilibrium morphology is maintained on removal of CO_2 strongly suggests a trapping mechanism. At some critical point during the polymerisation, when molecular weight exceeds the critical χN (which will be influenced by the presence of CO_2

and monomer), microphase separation takes place. We have developed a high pressure cell for future *in situ* monitoring of polymerisation and elucidation of the phase separation onset by SAXS.[47] Once all monomer is consumed, the final block copolymer morphology will be governed by the block volume fraction of CO_2-swollen PMMA relative to the 2nd block. On cooling the reaction, CO_2 remains between the polymer chains and morphology is arrested as both blocks pass below their T_g (lowered by CO_2 plasticisation) and chains cannot reorganise. Once CO_2 is removed from the polymerisation reactor, the morphology is unable to return to the thermodynamically favoured state based on polymer block volume fraction alone. Thus, the resulting morphology is kinetically-trapped and the CO_2 selective solvent effect persists.

Others have shown that RAFT dispersion polymerisation in aqueous or alcoholic media can be used to create a range of self-assembled structures (worms, vesicles, etc.)[48] but there are no published examples of microparticulate structures, as highlighted earlier.[22] Others have demonstrated formation of particles by heterogeneous CRP, but by use of emulsion and miniemulsion rather than dispersion, and all of these studies clearly produce only particles with lamellar morphologies at symmetric volume fractions[19, 49], or less well-defined morphologies that are trapped by crosslinking,[21] again demonstrating that the scCO_2 dispersion route is unusual.

Previous studies have found that non-equilibrium morphologies can be frozen into films of PS-*b*-PFOMA,[40] PS-*b*-PFMA[41, 50] and PDMS-*b*-PMPCS[42] after annealing in CO_2 (PFOMA, PFMA and PDMS are highly CO_2-philic blocks). Significantly, our data appear to be the first examples of CO_2 behaving as a block-selective solvent in block copolymers comprising only highly CO_2-phobic blocks. This effect might be enhanced by the confinement of block copolymer to microparticles rather than thin films which are typically studied. In thin films, there is the additional variable of polymer-substrate interaction. This can result in CO_2 concentration enrichment at the substrate relative to the polymer film,[51] which may reduce the influence of CO_2 on the block copolymer self-assembly. The ability to tune morphology as a function of polymer concentration in CO_2 hints at an alternative and facile method of influencing phase separated morphology of industrially relevant block copolymer particles.

Conclusions

We report detailed studies of the self-assembly of a number of block copolymers synthesised by RAFT-controlled dispersion polymerisation in $scCO_2$. Experimental phase diagrams for methacrylic-styrenic block copolymer systems differed from all-methacrylic systems in terms of the self-assembled morphologies at a range of block volume fractions. These data suggested that structural ambiguities result in differential absorption of CO_2 which leads to the formation of kinetically-trapped morphologies. This effect was confirmed by preparing bulk films under thermodynamic control, in which morphologies returned to those predicted by volume fraction, and the observed increase in domain size upon thermal annealing. Furthermore, by varying the ratio of polymer to CO_2, a morphological influence could be imparted by a selective solvent effect, which hints at an entirely new route to control nanostructured morphology of block copolymer particles in an already industrially-amenable synthetic process. The ability to create a range of morphologies from a single copolymer composition could be exploited for applications such as drug delivery vehicles, impact modifiers or even light scattering / light absorbing materials, in which properties will be dependent on internal nanostructured morphology.

Supporting Information

Block copolymer synthetic procedure, additional TEM images of block copolymer particles, raw SAXS data from block copolymer particles and films, SS NMR.

References

1. Schacher, F. H.; Rupar, P. A.; Manners, I., Functional Block Copolymers: Nanostructured Materials with Emerging Applications. *Angewandte Chemie-International Edition* **2012,** *51* (32), 7898-7921.
2. Bates, F. S., Polymer-Polymer Phase Behavior. *Science* **1991,** *251* (4996), 898-905.
3. Jinnai, H.; Nishikawa, Y.; Spontak, R. J.; Smith, S. D.; Agard, D. A.; Hashimoto, T., Direct measurement of interfacial curvature distributions in a bicontinuous block copolymer morphology. *Physical Review Letters* **2000,** *84* (3), 518-521; Vukovic, I.; Friedrich, H.; Merino, D. H.; Portale, G.; ten Brinke, G.; Loos, K., Shear-Induced Orientation of Gyroid PS-b-P4VP(PDP) Supramolecules. *Macromolecular Rapid Communications* **2013,** *34* (15), 1208-1212; Vukovic, I.; Voortman, T. P.; Merino, D. H.; Portale, G.; Hiekkataipale, P.; Ruokolainen, J.; ten Brinke, G.; Loos, K., Double Gyroid Network Morphology in Supramolecular Diblock Copolymer Complexes. *Macromolecules* **2012,** *45* (8), 3503-3512.
4. Chu, C. Y.; Jiang, X.; Jinnai, H.; Pei, R. Y.; Lin, W. F.; Tsai, J. C.; Chen, H. L., Real-space evidence of the equilibrium ordered bicontinuous double diamond structure of a diblock copolymer. *Soft Matter* **2015,** *11* (10), 1871-1876.

5. Voet, V. S. D.; Hermida-Merino, D.; ten Brinke, G.; Loos, K., Block copolymer route towards poly(vinylidene fluoride)/poly(methacrylic acid)/nickel nanocomposites. *Rsc Advances* **2013,** *3* (21), 7938-7946.
6. Olson, D. A.; Chen, L.; Hillmyer, M. A., Templating nanoporous polymers with ordered block copolymers. *Chem. Mat.* **2008,** *20* (3), 869-890.
7. Kang, Y.; Walish, J. J.; Gorishnyy, T.; Thomas, E. L., Broad-wavelength-range chemically tunable block-copolymer photonic gels. *Nature Materials* **2007,** *6* (12), 957-960.
8. Higuchi, T.; Tajima, A.; Motoyoshi, K.; Yabu, H.; Shimomura, M., Frustrated Phases of Block Copolymers in Nanoparticles. *Angewandte Chemie-International Edition* **2008,** *47* (42), 8044-8046.
9. Yabu, H.; Higuchi, T.; Jinnai, H., Frustrated phases: polymeric self-assemblies in a 3D confinement. *Soft Matter* **2014,** *10* (17), 2919-2931; Dobriyal, P.; Xiang, H. Q.; Kazuyuki, M.; Chen, J. T.; Jinnai, H.; Russell, T. P., Cylindrically Confined Diblock Copolymers. *Macromolecules* **2009,** *42* (22), 9082-9088.
10. Robb, M. J.; Connal, L. A.; Lee, B. F.; Lynd, N. A.; Hawker, C. J., Functional block copolymer nanoparticles: toward the next generation of delivery vehicles. *Polymer Chemistry* **2012,** *3* (6), 1618-1628.
11. Nykanen, A.; Rahikkala, A.; Hirvonen, S.-P.; Aseyev, V.; Tenhu, H.; Mezzenga, R.; Raula, J.; Kauppinen, E.; Ruokolainen, J., Thermally Sensitive Block Copolymer Particles Prepared via Aerosol Flow Reactor Method: Morphological Characterization and Behavior in Water. *Macromolecules* **2012,** *45* (20), 8401-8411.
12. Connal, L. A.; Lynd, N. A.; Robb, M. J.; See, K. A.; Jang, S. G.; Spruell, J. M.; Hawker, C. J., Mesostructured Block Copolymer Nanoparticles: Versatile Templates for Hybrid Inorganic/Organic Nanostructures. *Chem. Mat.* **2012,** *24* (21), 4036-4042.
13. Ku, K. H.; Kim, M. P.; Paek, K.; Shin, J. M.; Chung, S.; Jang, S. G.; Chae, W. S.; Yi, G. R.; Kim, B. J., Multicolor Emission of Hybrid Block Copolymer-Quantum Dot Microspheres by Controlled Spatial Isolation of Quantum Dots. *Small* **2013,** *9* (16), 2667-2672.
14. Yabu, H.; Jinno, T.; Koike, K.; Higuchi, T.; Shimomura, M., Three-Dimensional Assembly of Gold Nanoparticles in Spherically Confined Microphase-Separation Structures of Block copolymers. *Macromolecules* **2011,** *44* (15), 5868-5873.
15. Li, L.; Matsunaga, K.; Zhu, J.; Higuchi, T.; Yabu, H.; Shimomura, M.; Jinnai, H.; Hayward, R. C.; Russell, T. P., Solvent-Driven Evolution of Block Copolymer Morphology under 3D Confinement. *Macromolecules* **2010,** *43* (18), 7807-7812.
16. Higuchi, T.; Motoyoshi, K.; Sugimori, H.; Jinnai, H.; Yabu, H.; Shimomura, M., Phase transition and phase transformation in block copolymer nanoparticles. *Macromolecular Rapid Communications* **2010,** *31* (20), 1773-1778; Higuchi, T.; Shimomura, M.; Yabu, H., Reorientation of Microphase-Separated Structures in Water-Suspended Block Copolymer Nanoparticles through Microwave Annealing. *Macromolecules* **2013,** *46* (10), 4064-4068.
17. Lu, Z. H.; Liu, G. J.; Liu, F. T., Block copolymer microspheres containing intricate nanometer-sized segregation patterns. *Macromolecules* **2001,** *34* (25), 8814-8817.
18. Zhang, K.; Gao, L.; Chen, Y.; Yang, Z., Onion-like microspheres with tricomponent from gelable triblock copolymers. *Journal of Colloid and Interface Science* **2010,** *346* (1).
19. Kitayama, Y.; Kagawa, Y.; Minami, H.; Okubo, M., Preparation of micrometer-sized, onionlike multilayered block copolymer particles by two-step AGET ATRP in aqueous dispersed systems: Effect of the second-step polymerization temperature. *Langmuir* **2010,** *26* (10), 7029-7034.
20. Nicolas, J.; Ruzette, A.-V.; Farcet, C.; Gérard, P.; Magnet, S.; Charleux, B., Nanostructured latex particles synthesized by nitroxide-mediated controlled/living free-radical polymerization in emulsion. *Polymer* **2007,** *48* (24), 7029-7040.
21. Wei, R. Z.; Luo, Y. W.; Li, Z. S., Synthesis of structured nanoparticles of styrene/butadiene block copolymers via RAFT seeded emulsion polymerization. *Polymer* **2010,** *51* (17), 3879-3886.
22. Jennings, J.; Beija, M.; Richez, A. P.; Cooper, S. D.; Mignot, P. E.; Thurecht, K. J.; Jack, K. S.; Howdle, S. M., One-Pot Synthesis of Block Copolymers in Supercritical

Carbon Dioxide: A Simple Versatile Route to Nanostructured Microparticles. *J. Am. Chem. Soc.* **2012,** *134* (10), 4772-4781.
23. Jennings, J.; Beija, M.; Kennon, J. T.; Willcock, H.; O'Reilly, R. K.; Rimmer, S.; Howdle, S. M., Advantages of Block Copolymer Synthesis by RAFT-Controlled Dispersion Polymerization in Supercritical Carbon Dioxide. *Macromolecules* **2013,** *46* (17), 6843-6851.
24. Jixin, Y.; Hasell, T.; Smith, D. C.; Howdle, S. M., Deposition in supercritical fluids: from silver to semiconductors. *Journal of Materials Chemistry* **2009,** *19* (45), 8560-8570.
25. J. Brandrup; Immergut, E. H.; Grulke, E. A.; Abe, A.; Bloch, D. R., *Polymer Handbook* 4th ed.; John Wiley & Sons: 1999.
26. Spiess, H. W.; Schmidt-Rohr, K., *Multidimensional Solid-State NMR and Polymers,*. Academic Press Ltd.: London, 1994.
27. Clauss, J.; Schmidt-Rohr, K.; Spiess, H. W., DETERMINATION OF DOMAIN SIZES IN HETEROGENEOUS POLYMERS BY SOLID-STATE NMR. *Acta Polymerica* **1993,** *44* (1), 1-17.
28. Shao, Y.; Molnar, L. F.; Jung, Y.; Kussmann, J.; Ochsenfeld, C.; Brown, S. T.; Gilbert, A. T. B.; Slipchenko, L. V.; Levchenko, S. V.; O'Neill, D. P.; DiStasio, R. A., Jr.; Lochan, R. C.; Wang, T.; Beran, G. J. O.; Besley, N. A.; Herbert, J. M.; Lin, C. Y.; Van Voorhis, T.; Chien, S. H.; Sodt, A.; Steele, R. P.; Rassolov, V. A.; Maslen, P. E.; Korambath, P. P.; Adamson, R. D.; Austin, B.; Baker, J.; Byrd, E. F. C.; Dachsel, H.; Doerksen, R. J.; Dreuw, A.; Dunietz, B. D.; Dutoi, A. D.; Furlani, T. R.; Gwaltney, S. R.; Heyden, A.; Hirata, S.; Hsu, C.-P.; Kedziora, G.; Khalliulin, R. Z.; Klunzinger, P.; Lee, A. M.; Lee, M. S.; Liang, W.; Lotan, I.; Nair, N.; Peters, B.; Proynov, E. I.; Pieniazek, P. A.; Rhee, Y. M.; Ritchie, J.; Rosta, E.; Sherrill, C. D.; Simmonett, A. C.; Subotnik, J. E.; Woodcock, H. L., III; Zhang, W.; Bell, A. T.; Chakraborty, A. K.; Chipman, D. M.; Keil, F. J.; Warshel, A.; Hehre, W. J.; Schaefer, H. F., III; Kong, J.; Krylov, A. I.; Gill, P. M. W.; Head-Gordon, M., Advances in methods and algorithms in a modern quantum chemistry program package. *Physical Chemistry Chemical Physics* **2006,** *8* (27), 3172-3191.
29. Kitayama, Y.; Yorizane, M.; Minami, H.; Okubo, M., Preparation of block copolymer particles by two-step, reversible chain transfer catalyzed polymerization (RTCP) with nitrogen catalyst in miniemulsion systems. *Polymer Chemistry* **2012,** *3* (6), 1394-1398.
30. Guarini, K. W.; Black, C. T.; Yeuing, S. H. I., Optimization of diblock copolymer thin film self assembly. *Adv. Mater.* **2002,** *14* (18), 1290-+.
31. Ham, S.; Shin, C.; Kim, E.; Ryu, D. Y.; Jeong, U.; Russell, T. P.; Hawker, C. J., Microdomain orientation of PS-b-PMMA by controlled interfacial interactions. *Macromolecules* **2008,** *41* (17), 6431-6437.
32. Okubo, M.; Saito, N.; Takekoh, R.; Kobayashi, H., Morphology of poly styrene/polystyrene-block-poly(methyl methacrylate)/poly(methyl methacrylate) composite particles. *Polymer* **2005,** *46* (4), 1151-1156.
33. Wissinger, R. G.; Paulaitis, M. E., SWELLING AND SORPTION IN POLYMER-CO2 MIXTURES AT ELEVATED PRESSURES. *J. Polym. Sci. Pt. B-Polym. Phys.* **1987,** *25* (12), 2497-2510; Zhang, Y.; Gangwani, K. K.; Lemert, R. M., Sorption and swelling of block copolymers in the presence of supercritical fluid carbon dioxide. *J. Supercrit. Fluids* **1997,** *11* (1-2), 115-134; Hamedi, M.; Muralidharan, V.; Lee, B. C.; Danner, R. P., Prediction of carbon dioxide solubility in polymers based on a group-contribution equation of state. *Fluid Phase Equilib.* **2003,** *204* (1), 41-53.
34. Xuan, Y.; Peng, J.; Cui, L.; Wang, H. F.; Li, B. Y.; Han, Y. C., Morphology development of ultrathin symmetric diblock copolymer film via solvent vapor treatment. *Macromolecules* **2004,** *37* (19), 7301-7307.
35. Tanaka, T.; Saito, N.; Okubo, M., Control of Layer Thickness of Onionlike Multilayered Composite Polymer Particles Prepared by the Solvent Evaporation Method. *Macromolecules* **2009,** *42* (19), 7423-7429.
36. Lynd, N. A.; Meuler, A. J.; Hillmyer, M. A., Polydispersity and block copolymer self-assembly. *Prog. Polym. Sci.* **2008,** *33* (9), 875-893; Widin, J. M.; Kim, M.; Schmitt, A. K.; Han, E.; Gopalan, P.; Mahanthappa, M. K., Bulk and Thin Film Morphological Behavior

of Broad Dispersity Poly(styrene-b-methyl methacrylate) Diblock Copolymers. *Macromolecules* **2013,** *46* (11), 4472-4480.
37. Woods, H. M.; Silva, M.; Nouvel, C.; Shakesheff, K. M.; Howdle, S. M., Materials processing in supercritical carbon dioxide: surfactants, polymers and biomaterials. *Journal of Materials Chemistry* **2004,** *14* (11), 1663-1678; Curia, S.; de Focatiis, D. S. A.; Howdle, S. M., High-pressure rheological analysis of CO2-induced melting point depression and viscosity reduction of poly(epsilon-caprolactone). *Polymer* **2015,** *69*, 17-24; Pini, R.; Storti, G.; Mazzotti, M.; Tai, H.; Shakesheff, K. M.; Howdle, S. M., Sorption and swelling of poly(DL-lactic acid) and poly(lactic-co-glycolic acid) in supercritical CO2: An experimental and modeling study. *J. Polym. Sci. Pt. B-Polym. Phys.* **2008,** *46* (5), 483-496.
38. Vogt, B. D.; Brown, G. D.; RamachandraRao, V. S.; Watkins, J. J., Phase behavior of nearly symmetric polystyrene-block-polyisoprene copolymers in the presence of CO2 and ethane. *Macromolecules* **1999,** *32* (23), 7907-7912; Shinkai, T.; Ito, M.; Sugiyama, K.; Ito, K.; Yokoyama, H., Retrograde order-disorder transition of a semi-fluorinated block copolymer induced by supercritical carbon dioxide. *Soft Matter* **2013,** *9* (45), 10689-10693.
39. Vogt, B. D.; RamachandraRao, V. S.; Gupta, R. R.; Lavery, K. A.; Francis, T. J.; Russell, T. P.; Watkins, J. J., Phase behavior of polystyrene-block-poly(n-alkyl methacrylate)s dilated with carbon dioxide. *Macromolecules* **2003,** *36* (11), 4029-4036.
40. Li, Y.; Meli, L.; Lim, K. T.; Johnston, K. P.; Green, P. F., Structural inversion of micellar block copolymer thin films. *Macromolecules* **2006,** *39* (20), 7044-7054.
41. Yokoyama, H.; Li, L.; Dutriez, C.; Iwakura, Y.; Sugiyama, K.; Masunaga, H.; Sasaki, S.; Okuda, H., Horizontally and Vertically Aligned Polymeric Nanosheets: CO2-Induced Morphological Changes of Block Copolymer Thin Films. *Macromolecules* **2008,** *41* (22), 8626-8631.
42. Shi, L.-Y.; Shen, Z.; Fan, X.-H., Order-Order Transition in a Rod-Coil Diblock Copolymer Induced by Supercritical CO2. *Macromolecules* **2011,** *44* (8), 2900-2907.
43. Brus, J.; Urbanova, M.; Strachota, A., Epoxy networks reinforced with polyhedral oligomeric silsesquioxanes: Structure and segmental dynamics as studied by solid-state NMR. *Macromolecules* **2008,** *41* (2), 372-386.
44. Lodge, T. P.; Pudil, B.; Hanley, K. J., The full phase behavior for block copolymers in solvents of varying selectivity. *Macromolecules* **2002,** *35* (12), 4707-4717.
45. Hanley, K. J.; Lodge, T. P., Effect of dilution on a block copolymer in the complex phase window. *J. Polym. Sci. Pt. B-Polym. Phys.* **1998,** *36* (17), 3101-3113.
46. Kazarian, S. G.; Vincent, M. F.; Bright, F. V.; Liotta, C. L.; Eckert, C. A., Specific intermolecular interaction of carbon dioxide with polymers. *J. Am. Chem. Soc.* **1996,** *118* (7), 1729-1736.
47. Hermida-Merino, D.; Portale, G.; Fields, P.; Wilson, R.; Bassett, S. P.; Jennings, J.; Dellar, M.; Gommes, C.; Howdle, S. M.; Vrolijk, B. C. M.; Bras, W., A high pressure cell for supercritical CO2 on-line chemical reactions studied with x-ray techniques. *Review of Scientific Instruments* **2014,** *85* (9).
48. Sugihara, S.; Blanazs, A.; Armes, S. P.; Ryan, A. J.; Lewis, A. L., Aqueous Dispersion Polymerization: A New Paradigm for in Situ Block Copolymer Self-Assembly in Concentrated Solution. *Journal of the American Chemical Society* **2011,** *133* (39), 15707-15713; Zehm, D.; Ratcliffe, L. P. D.; Armes, S. P., Synthesis of Diblock Copolymer Nanoparticles via RAFT Alcoholic Dispersion Polymerization: Effect of Block Copolymer Composition, Molecular Weight, Copolymer Concentration, and Solvent Type on the Final Particle Morphology. *Macromolecules* **2013,** *46* (1), 128-139.
49. Kagawa, Y.; Minami, H.; Okubo, M.; Zhou, J., Preparation of block copolymer particles by two-step atom transfer radical polymerization in aqueous media and its unique morphology. *Polymer* **2005,** *46* (4), 1045-1049; Kitayama, Y.; Yorizane, M.; Kagawa, Y.; Minami, H.; Zetterlund, P. B.; Okubo, M., Preparation of onion-like multilayered particles comprising mainly poly-(iso-butyl methacrylate)-block-polystyrene by two-step AGET ATRP. *Polymer* **2009,** *50* (14), 3182-3187.

50. Shinkai, T.; Ito, M.; Sugiyama, K.; Ito, K.; Yokoyama, H., Ordered and foam structures of semifluorinated block copolymers in supercritical carbon dioxide. *Soft Matter* **2012,** *8* (21), 5811-5817.
51. O'Driscoll, B. M. D.; Griffiths, G. H.; Matsen, M. W.; Hamley, I. W., Structure Variation and Evolution in Microphase-Separated Grafted Diblock Copolymer Films. *Macromolecules* **2011,** *44* (21), 8527-8536.